UC San Diego
UC San Diego Previously Published Works

Title

Inflammatory hyperalgesia induces essential bioactive lipid production in the spinal cord

Permalink

https://escholarship.org/uc/item/6c13d3pz

Journal

Journal of Neurochemistry, 114(4)

ISSN

0022-3042

Authors

Buczynski, Matthew W
Svensson, Camilla I
Dumlao, Darren S
et al.

Publication Date

2010-08-01

DOI

10.1111/j.1471-4159.2010.06815.x

Peer reviewed

Inflammatory hyperalgesia induces essential bioactive lipid production in the spinal cord

Matthew W. Buczynski[1,†], **Camilla I. Svensson**[2,†,*], **Darren S. Dumlao**[1], **Bethany L. Fitzsimmons**[2], **Jae-Hang Shim**[2,3], **Thomas J. Scherbart**[1], **Faith E. Jacobsen**[1], **Xiao-Ying Hua**[2], **Tony L. Yaksh**[2,‡], and **Edward A. Dennis**[1,‡]

[1]Department of Pharmacology and Department of Chemistry and Biochemistry

[2]Department of Anesthesiology University of California San Diego, 9500 Gilman Drive, La Jolla, CA 92093

[3]Department of Ophthamology, Hanyang University College of Medicine, Seoul, Korea

Abstract

Lipid molecules play an important role in regulating the sensitivity of sensory neurons and enhancing pain perception, and growing evidence indicates that the effect occurs both at the site of injury and in the spinal cord. Using high-throughput mass spectrometry methodology, we sought to determine the contribution of spinal bioactive lipid species to inflammation-induced hyperalgesia in rats. Quantitative analysis of cerebrospinal fluid (CSF) and spinal cord tissue for eicosanoids, ethanolamides and fatty acids revealed the presence of 102 distinct lipid species. After induction of peripheral inflammation by intraplantar injection of carrageenan to the ipsilateral hind paw, lipid changes in cyclooxygenase (COX) and 12-lipoxygenase (12-LOX) signaling pathways peaked at 4 hours in the CSF. In contrast, changes occurred in a temporally disparate manner in the spinal cord with LOX-derived hepoxilins (HX) followed by COX-derived prostaglandin (PG) E_2, and subsequently the ethanolamine anandamide (AEA). Systemic treatment with the mu opioid agonist morphine, the COX inhibitor ketorolac, or the LOX inhibitor NDGA significantly reduced tactile allodynia, while their effects on the lipid metabolites were different. Morphine did not alter the lipid profile in the presence or absence of carrageenan inflammation. Ketorolac caused a global reduction in eicosanoid metabolism in naïve animals that remained suppressed following injection of carrageenan. NDGA-treated animals also displayed reduced basal levels of COX and 12-LOX metabolites, but only 12-LOX metabolites remained decreased after carrageenan treatment. These findings suggest that both COX and 12-LOX play an important role in the induction of carrageenan-mediated hyperalgesia through these pathways.

Introduction

The hallmark of persistent pain states following tissue injury and inflammation in humans and animals is increased sensitivity to subsequent stimulation. This hyperalgesia is mediated

‡To whom correspondence should be addressed. yaksh@ucsd.edu (T.L.Y.); edennis@ucsd.edu (E.A.D.).
†These authors contributed equally to this work
*Current address: Department of Physiology and Pharmacology, Karolinska Institute, Von Eulers vag 8, 171 77 Stockholm, Sweden

by both peripheral sensitization, a reduction in the threshold for activation of peripheral nociceptive sensory neurons, as well as spinal sensitization, an increase in the synaptic activity between sensory nerve endings and second-order neurons in the dorsal spinal cord. Centrally mediated spinal sensitization has been partially attributed to the bioactive lipid mediator PGE_2, which increases in CSF under a wide array of nociceptive models, including acute activation of small afferents (intraplantar formalin, heat) (Malmberg *et al.* 1995, Coderre *et al.* 1990, Shi *et al.* 2006) and persistent inflammation (Lucas *et al.* 2005, Shi et al. 2006, Svensson *et al.* 2003a, Svensson *et al.* 2005b, Svensson *et al.* 2003b, Yang *et al.* 1996a). Additionally, intrathecal administration of pro-nociceptive substances such as substance P, NMDA, kainate or cytokines (Yang *et al.* 1996b, Svensson *et al.* 2005a, Svensson et al. 2003a, Svensson et al. 2003b, Shi et al. 2006, Lucas et al. 2005, Svensson et al. 2005b) also modulate PGE_2 levels. From a pharmacological perspective, spinal PGE_2 production occurs via the COX enzyme, and can be prevented by COX inhibitors, which concurrently reduce the hyperalgesic state (Svensson & Yaksh 2002).

While PGE_2 is the most extensively studied, it represents only one of numerous bioactive lipid species that may play a role regulating spinal pain transmission. Eicosanoids comprise a class of hundreds of bioactive signaling lipids derived from the activity of COXs, LOXs and cytochrome P450s (CYP) on polyunsaturated fatty acids (Buczynski et al. 2009). In addition to PGE_2, other COX lipid products such as prostacyclin and PGD_2 demonstrate potential nociceptive modulatory capacity (Popp *et al.* 2009, Telleria-Diaz *et al.* 2008, Pulichino *et al.* 2006). Pathways other than the COX cascade have also been implicated in pain signaling, including 5-LOX (Cortes-Burgos et al. 2009), 12-LOX and 15-LOX products (Shin *et al.* 2002, Trang *et al.* 2004). CYP-derived epoxyeicosatrienoic acids (EETs) induce anti-hyperalgesia in murine pain models (Inceoglu *et al.* 2006, Inceoglu *et al.* 2008); endocannabinoids such as the N-acyl ethanolamine anandamide(AEA) can cause similar effects (Richardson *et al.* 1998, Tuboly *et al.* 2009).

Though a diverse range of lipid species formed in the spinal cord could potentially modulate nociceptive processing, only a handful have been studied in this context (Guay et al. 2004). We have now comprehensively assessed the presence and temporal release of eicosanoids and endocannabinoids in CSF and spinal cord parenchyma in a model of transient peripheral inflammation using high-throughput mass spectrometry methodology. Subsequently, we evaluated *in vivo* lipid changes following systemic pharmacological treatment to elucidate the role of these pathways.

Materials and Methods

Materials

LC grade solvents were purchased from EMD Biosciences. Synergy C18 reverse phase HPLC column and Strata-X solid phase extraction columns were purchased from Phenomenex (Torrance, CA). Eicosanoids were purchased from Cayman Chemicals (Ann Arbor, MI) and Biomol (Plymouth Meeting, PA). Ethanolamines were synthesized from fatty acid starting material or purchased from Cayman Chemicals when available. Fatty acids were purchased from Cayman Chemicals, Sigma Aldrich, and CDN Isotopes. Morphine sulfate (morphine) was provided by Merck (Rahway, NJ), ketorolac was provided

by Allergan (Irvine, CA), and nordihydroguaiaretic acid (NDGA) was purchased from Cayman Chemicals.

Ethanolamine Synthesis

The following eleven fatty acid ethanolamines were synthesized based on the procedure used by Abadji *et. al.* (Abadji et al. 1994): lauroyl (12:0)-EA, myristoyl (14:0)-EA, pentadecyloyl (15:0)-EA, heptadecyloyl (17:0)-EA, tricosanoyl (23:0)-EA, lignoceroyl (24:0)-EA, palmitoleoyl (16:1)-EA, erucinoyl (22:1)-EA, nervonoyl (24:1)-EA, γ-linolenoyl (18:3)-EA, eicosapentanoyl (20:5)-EA. Fatty acid was dissolved in THF converted into an acid chloride with oxalyl chloride, then reacted with ethanolamine to form the fatty acid ethanolamine. The product was purified by acid wash (1M HCl), base wash (1M $CaCO_3$), and a brine wash (1M NaCl), and recovered by recrystallization at 4°C for 24 h. For polyunsaturated fatty acid ethanolamines, recrystallization step was replaced by a Speed-Vac evaporation to a neat oil. The structure of the lipid products was confirmed by LC-MS, ^{1}H-NMR and elemental analysis.

Animals

Male Holtzman Sprague-Dawley rats (300-350 g; Harlan, Indianapolis, IN) were individually housed and maintained on a 12-h light/dark cycle with free access to food and water. All experiments were carried out according to protocols approved by the Institutional Animal Care Committee of University of California, San Diego.

Carrageenan Model of Hyperalgesia and Tactile Assessment

Carrageenan-induced inflammation in the rat paw represents a classical model of edema formation and hyperalgesia (Lucas et al. 2005, Svensson et al. 2005b). Carrageenan (100 μl, 2% (w/v) carrageenan dissolved in physiological saline) was injected subcutaneously to the plantar side of the right hind paw under light isoflurane anesthesia. Local inflammation was assessed by measurement of paw thickness using calipers. For measurement of tactile thresholds, rats were placed in individual Plexiglas compartments ($26 \times 11 \times 20$ cm) with wire mesh bottoms. Following a 30-min acclimation period, mechanical allodynia was assessed using von Frey filaments and the Dixon up-down method as described by Chaplan et al. (Chaplan et al. 1994). Briefly, calibrated filaments (Stoelting, Wood Dale, IL.) with buckling forces between 0.41 and 15.2 g were applied perpendicularly to the mid-paw plantar surface until the filament was slightly bent (L4 dermatome) and held there for 4-6 s. Stimuli were separated by several seconds or until the animal was calm with both hindpaws placed on the grid. The 50% probability withdrawal threshold was determined and plotted versus time; the data was also expressed as the area under the curve (AUC) of allodynic index for the time period 0-120 min. This resulting value has the units percentage change x time. The formula for calculating the percentage change is $100 \times$ (baseline tactile threshold - post-drug tactile threshold/baseline tactile threshold), where tactile threshold was expressed in grams. Increasing values indicates increasing tactile allodynia.

Drug Delivery

Drugs were delivered systemically (intraperitoneally, i.p.) in doses prepared in volumes of 0.5 ml/kg. Saline was used as a vehicle to deliver morphine (3 and 10 mg/kg) and ketorolac (30 mg/kg), whereas 10% cyclodextrin was used as a vehicle for NDGA (10 mg/kg). Drugs were administered 30 minutes prior to carrageenan injection. In the lipid profiling experiments the drugs were injected also at the 4 hour time point, immediately following the tactile threshold assessment.

Extraction of lipids from CSF and spinal cord tissue

For CSF extraction, isoflurane anesthetized rats were placed in the prone position and the spinous process at L1/L2 was identified as a tactile landmark. A midline skin incision, approximately 3 cm in length, was made caudally from the landmark to expose the interspinous space at L4/L5. The L4/L5 interspinous ligament and L5 spinous process were carefully removed. While elevating the L4 spinous process with forceps to widen the L4/L5 interlaminar space, the tip of a pulled capillary tube was obliquely introduced into the intrathecal space. The jugular veins were compressed to increase the intrathecal pressure and 40-50 μl of clear CSF was collected by capillary action. The volume was determined and the CSF then immediately mixed with 10% MeOH supplemented with internal standard. The lipids were extracted (see below) and stored at -20°C until analysis. Once the CSF was collected the rats were decapitated and the spinal cords removed from the vertebral column by hydroextrusion using a saline-filled syringe. The lumbar part of the spinal cord was dissected and split along the midline to allow analysis of the ipsilateral and contralateral sides separately. Tissue samples were stored at -80°C until lipid extraction.

Samples were placed in 600 ml of 10% MeOH and supplemented with 200 μL of internal standard, containing 50 pg/μL (2.5 ng total) of the following deuterated eicosanoids: (d_4) 6k $PGF_{1\alpha}$, (d_4) TXB_2, (d_4) $PGF_{2\alpha}$, (d_4) PGE_2, (d_4) PGD_2, (d_4) 15d PGJ_2, (d_{11}) 5-iso $PGF_{2\alpha}$ VI, (d_4) dhk $PGF_{2\alpha}$, (d_4) dhk PGD_2, (d_4) LTB_4, (d_8) 5-HETE, (d_8) 15-HETE, (d_6) 20-HETE, (d_4) 9-HODE, (d_4) 13-HODE, (d_7) 5-oxoETE, (d_8) 8,9-EET, (d_8) 11,12-EET, (d_8) 14,15-EET, (d_4) 9,10-diHOME, and (d_4) 12,13-diHOME; 50 pg/μL (2.5 ng total) of the following deuterated ethanolamines: (d_4) $PGF_{2\alpha}$,-EA, (d_4) palmitoyl(16:0)-EA, (d_4) oleoyl(18:1)-EA, and (d_4) arachidonoyl(20:4)-EA; and 100 pg/μL of the following deuterated fatty acids: (d_3) lauric(12:0) acid, (d_3) myristic(14:0) acid, (d_3) pentadecylic(15:0) acid, (d_3) palmitic(16:0) acid, (d_3) margaric(17:0) acid, (d_3) stearic(18:0) acid, (d_3) arachidic(20:0) acid, (d_3) behenic(22:0) acid, (d_4) lignoceric(24:0) acid, (d_4) cerotic(26:0) acid, (d_2) oleic(18:1) acid, (d_4) linoleic(18:2) acid, (d_8) arachidonic(20:4) acid, (d_5) eicosapentaenoic(20:5) acid, and (d_5) docosahexaenoic(22:6) acid.

Spinal cord tissue samples were sonicated for 30 seconds with a probe sonicator, and 80 μL was removed into 16 mm x 125 mm silica tubes for fatty acid extraction. The remaining sample was purified by solid phase extraction as previously described (Buczynski *et al.* 2007, Deems *et al.* 2007). Prior to eicosanoid LC-MS/MS analysis, samples were evaporated using a SpeedVac and reconstituted in 80 μL of LC Solvent A (water-acetonitrile-acetic acid (70:30:0.02; v/v/v)), with 40 μL injected on column. Following eicosanoid analysis, samples were supplemented with 10 μL of Solvent E (water-

acetonitrile-acetic acid-ammonium acetate (70:30:0.1; *v/v/v*) plus 5 mg/ml ammonium acetate) to match the sample solution constitution with LC Solvent C, and 40 μL was injected on column.

Fatty acids were extracted from samples as described by Zarini *el al.* (Zarini et al. 2006). Samples were supplemented with 200 μL of H_2O, 400 μL of MeOH and 20 μL of 1M HCl. Samples were then supplemented with 1.2 ml of iso-octane, vortexed for 30 sec, and centrifuged at 2000 rpm for 5 min. The upper (iso-octane) layer was removed and placed into a 75×15 silica tube. The iso-octane extraction was repeated twice, and stored at -20°C. Prior to analysis by GC-MS, samples were evaporated using a SpeedVac and derivatized using 25 μL of PFB (1% by volume in ACN) and 25 μL of TCICA (1% by volume in ACN). Samples were allowed to sit at room temperature for 30 min, evaporated by SpeedVac and reconstituted in 25 μL iso-octane for analysis, with 5 μL injected on column.

Liquid Chromatography and Mass Spectrometry of Eicosanoids

Eicosanoid analysis was performed by LC-MS/MS as previously described (Blaho et al. 2009). Briefly, eicosanoids were separated by a 25 min reverse-phase LC gradient using Solvent A [water-acetonitrile-acetic acid (70:30:0.02; v/v/v)] and solvent B [acetonitrile-isopropyl alcohol (50:50; v/v)]. Eicosanoids were subsequently analyzed using a tandem quadrupole mass spectrometer (ABI 4000 Q-Trap®, Applied Biosystems) via multiple-reaction monitoring (MRM) in negative-ion mode. Eicosanoids were identified in samples by matching their MRM signal and LC retention time with those of a pure standard.

Liquid Chromatography and Mass Spectrometry of Ethanolamines

Ethanolamines were separated by reverse-phase LC on a Luna C8 column (2.1 mm × 250 mm, 4u) at a flow rate of 300 μl/min at 50°C. The column was equilibrated in Solvent C [water-acetonitrile-acetic acid (70:30:0.02; v/v/v)], and 40 μl of sample was injected using a 50 μl injection loop and eluted with 0% solvent D [acetonitrile-isopropyl alcohol (50:50; v/v)] between 0 and 1 min. Solvent B was increased in a linear gradient to 25% solvent B until 3 min, to 45% until 11 min, to 60% until 13 min, to 75% until 18 min, and to 90% until 18.5 min. Solvent B was held at 90% until min 20, dropped to 0% by 21 min and held until 25 min. Ethanolamines were analyzed using a tandem quadrupole mass spectrometer (ABI 4000 Q-Trap®, Applied Biosystems) via multiple-reaction monitoring in positive-ion mode. The electrospray voltage was -4.5 kV, the turbo ion spray source temperature was 525°C. Collisional activation of eicosanoid precursor ions used nitrogen as a collision gas. Ethanolamines were measured using precursor→product multiple-reaction monitoring (MRM) pairs. The duty cycle was 930 ms, and the declustering potential and collision energy for each ethanolamine were optimized for maximal signal using flow injection mass spectrometry. Ethanolamines were identified in samples by matching their MRM signal and LC retention time with those of a pure standard.

Gas Chromatography and Mass Spectrometry of Fatty Acids

Fatty acids were analyzed by GC-MS as described by Zarini *et al.* (Zarini et al. 2006), whose work was expanded to cover additional fatty acids (Quehenberger et al. 2008). Fatty acids were separated using a gas chromatograph (Agilent 6890N, Hewlett Packard)

containing a 15 m (15 m × 0.25 mm inner diameter x 0.10 mm film thickness) Zebron dimethylpolysiloxane capillary column and analyzed by mass spectrometry. The injector temperature was maintained at 250°C and run in pulsed splitless mode, and the sample transfer line was maintained at 280°C. A constant flow of helium carrier gas was set at 0.9 ml/min. Fatty acids eluted with a temperature gradient starting at 150°C, increasing 10°C/min until 270°C, 40°C/min until 310°C and held for 1 min. Fatty acids were analyzed using a single quadrupole mass spectrometer (Agilent 5975, Hewlett Packard) via selected ion monitoring (SIM) in negative ion chemical ionization mode. Methane was used as the reagent gas. The source was maintained at 280°C and 200 eV, and the quadrupole was maintained at 150°C. Fatty acids were identified in samples by matching their SIM signal and GC retention time with those of a pure standard.

Quantitative and Qualitative Lipid Analysis

Quantitative lipid determination was performed by the stable isotope dilution method as previously described (Blaho et al. 2009, Deems et al. 2007). For eicosanoids and ethanolamines, 2.5 ng of each internal (deuterated) standard was mixed with the following amounts of natural (non-deuterated) primary standard: 0.1, 0.3, 1, 3, 10, 30 and 100 ng. For fatty acids, 25 ng of each internal (deuterated) standard was mixed with the following amounts of natural (non-deuterated) primary standard: 0.15, 0.5, 1.5, 5, 15, 50, 150 and 500 ng. Extraction controls were performed in quadruplicate and subtracted from each sample. The final values were normalized either to the weight of spinal cord tissue or the volume of CSF. Relative fold changes were determined using the (lipid:internal standard) ratio and expressed as a heat map, as described in detail here (Blaho et al. 2009).

Statistics

Statistical analysis was performed using SPSS (Version 17). All metabolite data was filtered using the Grubbs' test to remove outliers (Grubbs 1969). Results for the lipidomic array data are expressed as fold changes versus unstimulated rats (0 h) in the carrageenan time course study or versus vehicle-injected rats in the inhibitor studies, and displayed as a heat map. Individual metabolites and behavioral responses are expressed as the mean ± standard error of mean (s.e.m.), and statistical significance was determined by ANOVA with simple effects analysis or followed by the Dunnett's post-hoc test. Comparisons of heat map conditions were done by multiple analysis of variance (MANOVA) using Hotelling's T^2 test. For all tests, P values < 0.05 were considered significant.

Results

Basal levels of lipid mediators in rat CSF and spinal cord tissue

To determine the basal levels of spinal lipids, cerebrospinal fluid and the lumbar spinal cord were collected from naïve rats. Out of the 171 lipids detectable by our methodology, we identified 30 fatty acids, 22 ethanolamines, and 50 eicosanoids in either cerebral spinal fluid or spinal cord tissue homogenates from the naïve rats. The relative distributions of the species within each class are illustrated in Figure 1. In certain cases, contamination due to sample processing complicated the accurate measurement of lipid species from tissue samples, as explained below.

The spinal tissue contains a number of saturated, ω-9, ω-6 and ω-3 unsaturated free fatty acids. Of the total fatty acid content, saturated fatty acids accounted for over 60% by weight. Palmitic(16:0) and stearic(18:0) acid, which play an important role in energy metabolism, accounted for a significant portion of these lipids. Interestingly, lignoceric(24:0) acid was measured at levels roughly equivalent to palmitic(16:0), and significant quantities of behenic(22:0) and cerotic(26:0) acid were also detected. In comparison, the amounts of lauric(12:0) and myristic(14:0) acid are typically low; however, these lipids were identified as contaminants from plastic labware and prefabricated silica tubes utilized for sample processing, making them difficult to measure reproducibly. Within the unsaturated fatty acids, ω-6 Arachidonic(20:4) and ω-3 docosahexadecanoic(22:6) acid were the primary polyunsaturated fatty acids present in the spinal cord, though significant amounts of linolenic(18:3), DGLA(20:3), and adrenic(22:4) acid were also found in this tissue.

Of all the potential ethanolamines, only selected species have been synthesized and made commercially available. For this reason, it was important to first analyze spinal cord homogenates for any potential ethanolamine analogues from our fatty acid analysis. Ethananolamines are 43 amu larger than their corresponding fatty acid and typically fragment at the amide bond in positive ion mode. Thus, each potential ethanolamine corresponding with one of the 30 fatty acids species in the GC-MS analysis can be identified by LC-MS/MS with a series of $[M+43+H] \rightarrow 62$ multiple reaction monitoring transitions (Supplemental Figure 1). Commercially available standards were used to confirm the identity of known ethanolamines, and other unknown peaks potentially corresponding with a fatty acid ethanoamine were chemically synthesized to confirm their identity. In total, we identified and quantified 11 new metabolites that have not been previously characterized in spinal tissue (Supplemental Table 1).

Generally, the main fatty acids were also detected as ethanolamine species. The most abundant saturated species included palmitoyl(16:0) and stearoyl(18:0) ethanolamine; likewise, the oleoyl(18:1), arachidonoyl(20:4) and docosahexanoyl(22:6) ethanolamine were the most abundant unsaturated species. Similar to lauric(12:0) and myristic(14:0) acid, significant amounts of erucicoyl(22:1)-EA were identified as contaminant during sample processing. Arachidonic(20:4)-EA, known as anandamide (AEA), can be metabolized into eicosanoid ethanolamines, eicosanoid-like compounds generated through the COX, LOX, CYP and non-enzymatic pathways. We examined 13 eicosanoid ethanolamines, but at basal levels none of these metabolites were reproducibly found in significant quantities in spinal cord homogenates.

Numerous cyclooxygenase (COX), lipoxygenase (LOX), cytochrome P450 (CYP), and non-enzymatically derived metabolites were present in naïve rat spinal cord (Figure 1). COX metabolites directly produced by the five major prostaglandin synthases, as well as enzymatic (15k-PGE$_2$) and non-enzymatic (PGJ$_2$) breakdown metabolites were identified. Hydroxyeicosatetraenoic (HETE) and hydroxyoctadecaenoic (HODE) acids, lipoxygenase metabolites that modulate the activity of the peroxisome-proliferator activating factors (PPARs), also were found in spinal cord. Likewise, levels of CYP-derived epoxyeicosatrienoic (EET) acids and EpOMEs were approximately equivalent to their corresponding inactivated diols. In comparison with the spinal cord, the CSF contained

predominately arachidonic acid-derived prostaglandins (PG) and dihydroxyeicosatrienoic acids (DHET), with ethanolamine levels registering below the limit of detection.

Carrageenan induces inflammatory hyperalgesia and lipid changes in CSF and spinal tissues

We assessed both nociceptive behavior and spinal lipid alteration in the carrageenan model. Changes in hypersensitivity following carrageenan injection were determined by assessment of tactile allodynia (Figure 2). The tactile threshold rapidly decreased progressively subsequent to carrageenan injection, reaching maximal allodynia between two and four hours. The hypersensitivity persisted for approximately 24 hours with tactile thresholds returning to baseline after 72 hours post-injection, meanwhile the contralateral paw withdrawal thresholds remained unchanged. Based on this time profile, we focused on the first 24 hours in order to identify endogenous spinal ethanolamines and eicosanoids that may play a role in the induction and maintenance of hyperalgesia.

Lipid changes in the spinal cord and CSF following induction of inflammation were assessed and correlated with the behavioral changes (see Figures 3-5). The major lipid metabolites increased in CSF in response to carrageenan arose through the COX pathway, including PGE_2 and the prostacyclin stable metabolite 6k $PGF_{1\alpha}$, as well as 12-HETE from the 12-LOX pathway. Interestingly, changes in the metabolite levels in the CSF did not directly mirror those occurring in the neural microenvironment of the spinal parenchyma, with each of these loci displaying a unique lipidomic fingerprint (Figure 3). Generally, lipid changes in the CSF occurred more rapidly and to a greater magnitude, whereas spinal tissue changes were more subtle, and sustained for a greater period of time. The majority of lipid changes we observed resulted from increased levels, with only a few sporadic metabolites diminishing after carrageenan.

Multiple analysis of variance (MANOVA) was utilized as a preliminary screen for possible pathway-specific perturbations. To investigate potential differences in a given pathway between each side of the spinal cord, the interaction of tissue, time and metabolite between the ipsilateral and contralateral tissue was analyzed by three-way MANOVA (Table 1). This analysis did not identify significant differences between the ipsilateral and contralateral spinal cord in the COX or LOX pathways; however, we did observe potential differences in the saturated ethanolamines as well as the CYP pathway. In these sets, each metabolite (within a given tissue) was analyzed by ANOVA followed by the Dunnett's posthoc test, where each time point compared to time 0h; additionally, each metabolite (within a given time point) from the ipsilateral and contralateral tissue was analyzed by ANOVA followed by a significant effects analysis. Heptadecyloyl (17:0)-EA accounted for saturated ethanolamine differences between these tissues, with ANOVA identifying a single temporal alteration in the ipsilateral (2 h) and contralateral (18 h) sides. ANOVA of CYP temporal changes failed to uncover any significant changes compared with 0 h within either the ipsilateral or contralateral tissue. However, simple effects analysis revealed increased EET production on the contralateral side when compared to the ipsilateral counterpart (Figure 4), with both 8,9-EET and 11,12-EET demonstrating differences at 2 h , 4 h, 12 h and 24 h.

To systematically identify other temporal changes, two-way MANOVA screened for changes in either the CSF or ipsilateral spinal cord in response to carrageenan injury (Table 1). This screen failed to detect any alterations in either 5-LOX or ω-9 ethanolamines; other classes were further investigated using previously described ANOVA analyses. In the CSF, PGE_2 levels increased at 4 h, then gradually returned to basal levels (Figure 5); a pattern was observed for the stable prostacyclin metabolite 6k-$PGF_{1\alpha}$ and the 12-LOX metabolite 12-HETE. There was a time dependent increase in the PGE_2 level in the ipsilateral spinal tissue that started at four hours, with statistically significant increases at 8h, 12h, and 18h. Regarding the 12-LOX pathway, HXB_3 levels trended upward immediately following peripheral injury, and significantly increased at 8h and 18h. While the hepoxilin synthase creates both HXA_3 and HXB_3, the conditions of our assay system degrade HXA_3 and hence we used HXB_3 as a marker of hepoxilin synthase activity. We observed delayed production in spinal levels of AEA, beginning after 4 h and demonstrating statistical significance at 18 h and 24 h. Comparison of these metabolites in the ipsilateral versus the contralateral side confirmed the bilaterality of these metabolites, identifying no dissimilarity in AEA levels, and only one difference in the levels of HXB_3 (0 h, $p = 0.036$) and PGE_2 (4 h, $p = 0.025$). The complete quantitative analysis of the other ethanolamine and eicosanoid lipid species is available in as supplemental information (Supplemental Table 3-5).

Effects of Morphine, Ketorolac and NDGA on hyperalgesia and spinal lipid metabolites

We examined the effect of systemic injection of morphine (3 mg/kg and 10 mg/kg), ketorolac (30 mg/kg) and NDGA (10 mg/kg) on tactile thresholds (0-4 h) and spinal lipid metabolites (at 8 h time point) in the presence and absence of carrageenan inflammation (Figure 6-8). Morphine is a mu-opiate receptor agonist, producing analgesia via blockage of nociceptive transmission at the spinal and superspinal levels; at the concentrations used in this study, it had no effect on locomotor activity (unpublished observations). Ketorolac is a non-selective COX-1/2 inhibitor, with no demonstrable activity on lipoxygenases (Handley et al. 1998) or other receptors involved in central mechanisms of analgesia (Jett *et al.* 1999). NDGA acts as a general LOX inhibitor, with preferential binding to 12-LOXs but with no demonstrable effect on cyclooxygenase (Handley et al. 1998, Argentieri *et al.* 1994). These three drugs, given to rats 30 min prior to carrageenan injection, all displayed potent antihyperalgesic effects on carrageenan induced tactile hypersensitivity at the examined doses (Figure 6). We measured the paw thickness (swelling) to assess the effects of these inhibitors on the local inflammation caused by carrageenan. In the vehicle-treated group, the diameter of the ipsilateral paw was doubled 7 hours after carrageenan (before, 5.8 ± 0.6 mm, after 11.5 ± 0.2 mm, $p < 0.05$), suggesting pronounced local inflammation (Supplemental Figure 2). Morphine and NDGA treatment had no effect on the amount of swelling in the ipsilateral hindpaw. While ketorolac attenuated paw swelling by 20%, the overall carrageenan-induced peripheral inflammation in the presence of this inhibitor remained significant.

To demonstrate the effect of treatment on spinal eicosanoid metabolites, levels of PGE_2, HXB_3, and AEA were measured in both control and carrageenan-injected animals (Figure 7). Systemic pretreatment with morphine did not have any significant effect on these metabolite levels in either control or carrageenan-injected rats, indicating that its

antinociceptive mechanism works independently of eicosanoid signaling. Both ketorolac and NDGA reduced the resting levels of PGE_2. Ketorolac also prevented carrageenan-induced increases in PGE_2, whereas NDGA did not inhibit spinal PGE_2 production in this model. The basal levels of HXB_3 and AEA were both reduced by treatment with either ketorolac or NDGA, and these reductions were sustained in carrageenan-treated animals. Interestingly, whereas inhibition of COX by ketorolac also affects 12-LOX production of HXB_3 under basal and inflammatory conditions, the inhibition of LOX by NDGA does not block the carrageenan-induced PGE_2 increase.

Accordingly, aglobal assessment of the lipid changes was performed (Figure 8). Morphine did not alter the spinal lipid profile, confirming that mu-opioid receptors do not mediate carrageenan-induces changes in spinal lipid biosynthesis. As expected, ketorolac and NDGA blocked respectively COX and 12-LOX downstream mediators; however, they also produced a number of unforeseen changes. Ketorolac treatment, in addition to blocking COX activity, profoundly reduced the basal levels of most LOX and CYP metabolites in our assay, as well as carrageenan-induced synthesis of these lipids. NDGA also caused a reduction in the basal levels of these metabolites, but upon insult with carrageenan the levels of most COX and non-enzymatically derived eicosanoids returned back to the levels of the control group (i.e. carrageenan rats with vehicle treatment). Only a small number of the bioactive lipid metabolites detected in this study increased following inhibitor treatment, primarily the saturated fatty acids such as palmitic(16:0) and stearic(18:0) acid (Figure 9). With the exception of NDGA in naïve rats, arachidonic acid levels remained unchanged following treatment in both naïve and carrageenan animals. This illustrates that following inhibitor treatment, AA is neither metabolically shunted into other biosynthetic pathways nor does it accumulate in the tissue following carrageenan injection. Quantitative assessments of each individual metabolite are available as supplemental information (Supplemental Table 6).

Discussion

In the current work, we identified 102 distinct fatty acid, ethanolamine and eicosanoid species in the spinal fluid and parenchyma of naïve animals. Peripheral injection of carrageenan induced an increase in tactile hypersensitivity, which correlated with spinal upregulation of COX, 12-LOX, CYP and ethanolamine metabolites. While the lipoxygenase pathway contained both the greatest number of species and the highest level of abundance, these metabolites did not originate from the classic pro-inflammatory 5-LOX pathway but from the 12-LOX pathway. The changes in spinal lipid levels were unaffected by morphine pre-treatment, demonstrating that mu opioid receptors do not regulate the spinal production of pro-hyperalgesic lipid metabolites. However, systemic administration of ketorolac or NDGA blocked COX- and LOX-derived lipid production, respectively. Interestingly, both ketorolac and NDGA indirectly modulated eicosanoids outside their intended metabolic pathways and reduced spinal AEA levels. Taken together, these pathways may interact during nociceptive signaling and have important therapeutic implications.

Each of the drugs utilized in this study significantly reduced tactile allodynia but, as mentioned above, had different effects on the spinal lipid profile. Ketorolac reduced COX

products such as PGE$_2$, but also decreased 12-LOX synthesized hepoxilins and a number of other metabolites from the LOX and CYP pathways. NDGA reduced the basal levels of COX, LOX and CYP metabolites; however, while the COX metabolites returned to vehicle levels following administration of carrageenan, LOX levels remained depressed. Ketorolac and NDGA both diminished AEA levels as well as increasing saturated fatty acids in the spinal cord. These effects suggested that different arms of the eicosanoid biosynthetic pathway may exhibit cross-talk as opposed to shunting. The shunting model for inhibition would suggest that following inhibition of an eicosanoid biosynthetic enzyme, the substrate (i.e. arachidonic acid) can be shunted into another pathway and increase those metabolites. However, our data demonstrate that arachidonic acid levels either rose or remain unaltered when eicosanoid levels dropped following COX or LOX inhibition. On the other hand, cross-talk between these pathways could explain how the loss of one eicosanoid signal could affect the activity of other cells and thus modulate eicosanoid biosynthetic pathways. For example, the loss of COX-derived PGE$_2$ in the CNS could negatively regulate the activity of cells dirercly producing spinal 12-LOX metabolites, culminating in diminished levels. Alternatively, PGE$_2$ produced at the peripheral site of carrageenan injury could alter noceceptive signaling that drive the spinal eicosanoid changes by activating COX and 12-LOX in the CNS. Future experiments utilizing locally administered inhibitors, both in the injured paw as well as the intrathecal space, will help further elucidate these interactions.

No differences in levels of COX, LOX, or ethanolamine metabolites were observed between ipsilateral and contralateral lumbar samples. This compliments work showing bilateral changes in COX-2 levels in response to peripheral carrageenan injection (Pham-Marcou et al. 2008), and opens critical questions regarding the origin of the lipid metabolites and the role they play in the unilateral manifestation of hypersensitivity. It is unlikely that spinal lipid changes can be attributed to peripheral eicosanoids traveling to the spinal tissue from the systemic circulation. Intravenous injection of PGE$_2$ rapidly (less than 90 seconds) metabolizes into dhk PGE$_2$, the primary metabolite in human blood (Hamberg & Samuelsson 1971); in our study, spinal dhk PGE$_2$ is nearly undetectable and PGE$_2$ is the predominant metabolite strongly suggesting a limited direct contribution from blood products. Thus, two possible sites of origin exist; the lipids may come from the endothelial cells in the spinal vasculature or from glial and/or neuronal cells within the CNS.

Peripheral inflammation leads to increases in circulating cytokines which, although unable to cross the blood-brain barrier (BBB), could increase eicosanoid levels in neural tissues by activating the vascular endothelium or perivascular non-neuronal cells (Engblom et al. 2002). Although the local site of inflammation contains pro-inflammatory TNF$_\alpha$ and IL-1β, these cytokines do not increase in plasma following carrageenan-injection (Huber *et al.* 2006, Loram *et al.* 2007), indicating a local containment of the inflammatory process in the hindpaw. Oka *et. al.* reported increases of IL-6 in serum following carrageenan injection, which induced COX-2 protein expression within CNS endothelial cells (Oka *et al.* 2007, Ibuki *et al.* 2003). In contrast, Loram *et. al.* failed to detect serum IL-6 changes in the same model but instead identified CINC-1, another cytokine implicated in the development of hyperalgesia (Loram et al. 2007). In addition to COX-2, endothelial cells also express 12-LOX and CYP proteins which have demonstrable eicosanoid biosynthetic capacity (Kim *et*

al. 1995, Nie *et al.* 2000, Liu *et al.* 2005). Hence, though a specific circulating cytokine has not been conclusively identified, it is possible that several of the arachidonic acid metabolites found in CSF and spinal parenchyma originate from endothelial cells in response to circulating inflammatory mediators.

Alternatively, the lipid mediators found in CSF and spinal cord samples could result from spinal neuronal excitability driving local synthesis. In support of this possibility, elevated levels of TNF_α have been measured in CSF and the spinal cord following local peripheral inflammation despite a lack of increase in plasma (Bianchi et al. 2007). Local anesthetics block carrageenan-induced bilateral increases in spinal TNF_α and COX-2 expression (Beloeil *et al.* 2009, Beloeil *et al.* 2006). Interestingly, local anesthetics also block carrageenan evoked increases BBB permeability, indicating a connection between central nociceptive signaling and the BBB (Campos et al. 2008). Some of the lipid mediators identified in current work could mediate this connection, an intriguing possibility that warrants further studies.

Lipoxygenase involvement in pain research has focused primarily on 5-LOX. Peripheral inflammation is heavily influenced by leukotriene signaling, and systemic administration of zileuton, a 5-LOX selective inhibitor, has been shown to reduce carrageenan-induced hyperalgesia (Singh *et al.* 2005, Cortes-Burgos et al. 2009). However, to date no one has assessed the involvement of 5-LOX at the spinal level and our data do not demonstrate any evidence of 5-LOX signaling in spinal tissue. Instead, our results suggest a stronger influence of 12-LOX in mediating spinal nociception. Other work has previously implicated 12-HpETE (often assayed as 12-HETE) as a potential hyperalgesic signal operating through TRPV1 (Shin et al. 2002), and here we propose that hepoxilins could also play an important role. While the precise roles of hepoxilins have not been elucidated in the spinal cord, they have been suggested as potentiators of neurite regeneration after nerve injury and to play a global role in calcium regulation. Intriguingly, HXA_3 displayed excitatory effects when applied to hippocampal neurons (Carlen *et al.* 1989, Amer *et al.* 2003). However, numerous challenges impede further investigation of 12-LOX signaling. Five distinct potential 12-LOX genes have been identified to date, each with isoform- and species-selective catalytic properties that have not been thoroughly investigated in rodents (Buczynski et al. 2009). A model of peripheral joint inflammation demonstrated distinct temporal changes in hepoxilin and 12-HETE levels within the joint (Blaho et al. 2009), raising the possibility that each 12-LOX isoform plays a unique physiological roles. Along this line, our work identified increased 12-HETE in the CSF whereas hepoxilin changes only occurred in the spinal tissue. Though progress has been made toward the development of isoform-selective 12-LOX inhibitors (Kenyon *et al.* 2006, Deschamps *et al.* 2007, van Leyen *et al.* 2008), this critical issue remains largely unresolved.

Though COX, LOX, and ethanolamine biosynthesis occurs bilaterally, hyperalgesia manifests itself ipsilaterally, suggesting the presence of factor(s) that either cause ipsilateral or prevent contralateral hypersensitivity. Within the scope of our lipidomic screen, we identified anti-hyperalgesic CYP-derived EETs as a candidate. Preliminary evidence indicates EETs have anti-nociceptive effects (Inceoglu et al. 2008, Inceoglu et al. 2006), and our data suggests that some mechanism either induces their contralateral biosynthesis or

suppresses their ipsilateral induction following peripheral injury. In addition, recent work demonstrates that carrageenan induces unilateral Fos expression that occurs in a lipoxygenase dependent manner (Yoo et al. 2009). Systemic administration of analgesic doses of morphine also reduces Fos expression (Honore et al. 1996), which our data shows does not regulate spinal eicosanoid production. This suggests a potential target for the intersection between bilateral eicosanoids and unilateral primary afferent nociceptive signaling. Future investigations should focus on the specific roles of endogenous COX, 12-LOX, CYP, and anandamide signaling in the central nervous system. Understanding these mechanisms will uncover novel targets such as 12-LOX which may be modulated pharmacologically for the management of inflammatory pain.

Supplementary Material

Refer to Web version on PubMed Central for supplementary material.

Acknowledgments

References

Abadji V, Lin S, Taha G, Griffin G, Stevenson LA, Pertwee RG, Makriyannis A. (R)-methanandamide: a chiral novel anandamide possessing higher potency and metabolic stability. J Med Chem. 1994; 37:1889–1893. [PubMed: 8021930]

Amer RK, Pace-Asciak CR, Mills LR. A lipoxygenase product, hepoxilin A(3), enhances nerve growth factor-dependent neurite regeneration post-axotomy in rat superior cervical ganglion neurons in vitro. Neuroscience. 2003; 116:935–946. [PubMed: 12617935]

Argentieri DC, Ritchie DM, Ferro MP, Kirchner T, Wachter MP, Anderson DW, Rosenthale ME, Capetola RJ. Tepoxalin: a dual cyclooxygenase/5-lipoxygenase inhibitor of arachidonic acid metabolism with potent anti-inflammatory activity and a favorable gastrointestinal profile. J Pharmacol Exp Ther. 1994; 271:1399–1408. [PubMed: 7996452]

Beloeil H, Gentili M, Benhamou D, Mazoit JX. The effect of a peripheral block on inflammation-induced prostaglandin E2 and cyclooxygenase expression in rats. Anesth Analg. 2009; 109:943–950. [PubMed: 19690271]

Beloeil H, Ji RR, Berde CB. Effects of bupivacaine and tetrodotoxin on carrageenan-induced hind paw inflammation in rats (Part 2): cytokines and p38 mitogen-activated protein kinases in dorsal root ganglia and spinal cord. Anesthesiology. 2006; 105:139–145. [PubMed: 16810005]

Bianchi M, Martucci C, Ferrario P, Franchi S, Sacerdote P. Increased tumor necrosis factor-alpha and prostaglandin E2 concentrations in the cerebrospinal fluid of rats with inflammatory hyperalgesia: the effects of analgesic drugs. Anesth Analg. 2007; 104:949–954. [PubMed: 17377112]

Blaho VA, Buczynski MW, Brown CR, Dennis EA. Lipidomic Analysis of Dynamic Eicosanoid Responses During the Induction and Resolution of Lyme Arthritis. J Biol Chem. 2009

Buczynski MW, Dumlao DS, Dennis EA. Thematic Review Series: Proteomics. An integrated omics analysis of eicosanoid biology. J Lipid Res. 2009; 50:1015–1038. [PubMed: 19244215]

Buczynski MW, Stephens DL, Bowers-Gentry RC, Grkovich A, Deems RA, Dennis EA. TLR-4 and sustained calcium agonists synergistically produce eicosanoids independent of protein synthesis in RAW264.7 cells. J Biol Chem. 2007; 282:22834–22847. [PubMed: 17535806]

Campos CR, Ocheltree SM, Hom S, Egleton RD, Davis TP. Nociceptive inhibition prevents inflammatory pain induced changes in the blood-brain barrier. Brain Res. 2008; 1221:6–13. [PubMed: 18554577]

Carlen PL, Gurevich N, Wu PH, Su WG, Corey EJ, Pace-Asciak CR. Actions of arachidonic acid and hepoxilin A3 on mammalian hippocampal CA1 neurons. Brain Res. 1989; 497:171–176. [PubMed: 2507088]

Chaplan SR, Bach FW, Pogrel JW, Chung JM, Yaksh TL. Quantitative assessment of tactile allodynia in the rat paw. J Neurosci Methods. 1994; 53:55–63. [PubMed: 7990513]

Coderre TJ, Gonzales R, Goldyne ME, West J, Levine JD. Noxious stimulus-induced increase in spinal prostaglandin E2 is noradrenergic terminal-dependent. Neurosci Lett. 1990; 115:253–258. [PubMed: 2122330]

Cortes-Burgos LA, Zweifel BS, Settle SL, et al. CJ-13610, an orally active inhibitor of 5-lipoxygenase is efficacious in preclinical models of pain. Eur J Pharmacol. 2009

Deems R, Buczynski MW, Bowers-Gentry R, Harkewicz R, Dennis EA. Detection and quantitation of eicosanoids via high performance liquid chromatography-electrospray ionization-mass spectrometry. Methods Enzymol. 2007; 432:59–82. [PubMed: 17954213]

Deschamps JD, Gautschi JT, Whitman S, Johnson TA, Gassner NC, Crews P, Holman TR. Discovery of platelet-type 12-human lipoxygenase selective inhibitors by high-throughput screening of structurally diverse libraries. Bioorg Med Chem. 2007; 15:6900–6908. [PubMed: 17826100]

Engblom D, Ek M, Saha S, Ericsson-Dahlstrand A, Jakobsson PJ, Blomqvist A. Prostaglandins as inflammatory messengers across the blood-brain barrier. J Mol Med. 2002; 80:5–15. [PubMed: 11862319]

Grubbs FE. Procedures for Detecting Outlying Observations in Samples. Technometrics. 1969; 11:1.

Guay J, Bateman K, Gordon R, Mancini J, Riendeau D. Carrageenan-induced paw edema in rat elicits a predominant prostaglandin E2 (PGE2) response in the central nervous system associated with the induction of microsomal PGE2 synthase-1. J Biol Chem. 2004; 279:24866–24872. [PubMed: 15044444]

Hamberg M, Samuelsson B. On the metabolism of prostaglandins E 1 and E 2 in man. J Biol Chem. 1971; 246:6713–6721. [PubMed: 5126221]

Handley DA, Cervoni P, McCray JE, McCullough JR. Preclinical enantioselective pharmacology of (R)- and (S)- ketorolac. J Clin Pharmacol. 1998; 38:25S–35S. [PubMed: 9549656]

Honore P, Buritova J, Besson JM. The effects of morphine on carrageenin-induced spinal c-Fos expression are completely blocked by beta-funaltrexamine, a selective mu-opioid receptor antagonist. Brain Res. 1996; 732:242–246. [PubMed: 8891291]

Huber JD, Campos CR, Mark KS, Davis TP. Alterations in blood-brain barrier ICAM-1 expression and brain microglial activation after lambda-carrageenan-induced inflammatory pain. Am J Physiol Heart Circ Physiol. 2006; 290:H732–740. [PubMed: 16199477]

Ibuki T, Matsumura K, Yamazaki Y, Nozaki T, Tanaka Y, Kobayashi S. Cyclooxygenase-2 is induced in the endothelial cells throughout the central nervous system during carrageenan-induced hind paw inflammation; its possible role in hyperalgesia. J Neurochem. 2003; 86:318–328. [PubMed: 12871573]

Inceoglu B, Jinks SL, Schmelzer KR, Waite T, Kim IH, Hammock BD. Inhibition of soluble epoxide hydrolase reduces LPS-induced thermal hyperalgesia and mechanical allodynia in a rat model of inflammatory pain. Life Sci. 2006; 79:2311–2319. [PubMed: 16962614]

Inceoglu B, Jinks SL, Ulu A, et al. Soluble epoxide hydrolase and epoxyeicosatrienoic acids modulate two distinct analgesic pathways. Proc Natl Acad Sci U S A. 2008; 105:18901–18906. [PubMed: 19028872]

Jett MF, Ramesha CS, Brown CD, et al. Characterization of the analgesic and anti-inflammatory activities of ketorolac and its enantiomers in the rat. J Pharmacol Exp Ther. 1999; 288:1288–1297. [PubMed: 10027870]

Kenyon V, Chorny I, Carvajal WJ, Holman TR, Jacobson MP. Novel human lipoxygenase inhibitors discovered using virtual screening with homology models. J Med Chem. 2006; 49:1356–1363. [PubMed: 16480270]

Kim JA, Gu JL, Natarajan R, Berliner JA, Nadler JL. A leukocyte type of 12-lipoxygenase is expressed in human vascular and mononuclear cells. Evidence for upregulation by angiotensin II. Arterioscler Thromb Vasc Biol. 1995; 15:942–948. [PubMed: 7600127]

Liu Y, Zhang Y, Schmelzer K, et al. The antiinflammatory effect of laminar flow: the role of PPARgamma, epoxyeicosatrienoic acids, and soluble epoxide hydrolase. Proc Natl Acad Sci U S A. 2005; 102:16747–16752. [PubMed: 16267130]

Loram LC, Fuller A, Fick LG, Cartmell T, Poole S, Mitchell D. Cytokine profiles during carrageenan-induced inflammatory hyperalgesia in rat muscle and hind paw. J Pain. 2007; 8:127–136. [PubMed: 16949880]

Lucas KK, Svensson CI, Hua XY, Yaksh TL, Dennis EA. Spinal phospholipase A2 in inflammatory hyperalgesia: role of group IVA cPLA2. Br J Pharmacol. 2005; 144:940–952. [PubMed: 15685208]

Malmberg AB, Hamberger A, Hedner T. Effects of prostaglandin E2 and capsaicin on behavior and cerebrospinal fluid amino acid concentrations of unanesthetized rats: a microdialysis study. J Neurochem. 1995; 65:2185–2193. [PubMed: 7595506]

Nie D, Tang K, Diglio C, Honn KV. Eicosanoid regulation of angiogenesis: role of endothelial arachidonate 12-lipoxygenase. Blood. 2000; 95:2304–2311. [PubMed: 10733500]

Oka Y, Ibuki T, Matsumura K, Namba M, Yamazaki Y, Poole S, Tanaka Y, Kobayashi S. Interleukin-6 is a candidate molecule that transmits inflammatory information to the CNS. Neuroscience. 2007; 145:530–538. [PubMed: 17303338]

Pham-Marcou TA, Beloeil H, Sun X, Gentili M, Yaici D, Benoit G, Benhamou D, Mazoit JX. Antinociceptive effect of resveratrol in carrageenan-evoked hyperalgesia in rats: prolonged effect related to COX-2 expression impairment. Pain. 2008; 140:274–283. [PubMed: 18814970]

Popp L, Haussler A, Olliges A, Nusing R, Narumiya S, Geisslinger G, Tegeder I. Comparison of nociceptive behavior in prostaglandin E, F, D, prostacyclin and thromboxane receptor knockout mice. Eur J Pain. 2009; 13:691–703. [PubMed: 18938093]

Pulichino AM, Rowland S, Wu T, Clark P, Xu D, Mathieu MC, Riendeau D, Audoly LP. Prostacyclin antagonism reduces pain and inflammation in rodent models of hyperalgesia and chronic arthritis. J Pharmacol Exp Ther. 2006; 319:1043–1050. [PubMed: 16973887]

Quehenberger O, Armando A, Dumlao D, Stephens DL, Dennis EA. Lipidomics analysis of essential fatty acids in macrophages. Prostaglandins Leukot Essent Fatty Acids. 2008; 79:123–129. [PubMed: 18996688]

Richardson JD, Aanonsen L, Hargreaves KM. Antihyperalgesic effects of spinal cannabinoids. Eur J Pharmacol. 1998; 345:145–153. [PubMed: 9600630]

Shi L, Smolders I, Umbrain V, Lauwers MH, Sarre S, Michotte Y, Zizi M, Camu F. Peripheral inflammation modifies the effect of intrathecal IL-1beta on spinal PGE2 production mainly through cyclooxygenase-2 activity. A spinal microdialysis study in freely moving rats. Pain. 2006; 120:307–314. [PubMed: 16427196]

Shin J, Cho H, Hwang SW, et al. Bradykinin-12-lipoxygenase-VR1 signaling pathway for inflammatory hyperalgesia. Proc Natl Acad Sci U S A. 2002; 99:10150–10155. [PubMed: 12097645]

Singh VP, Patil CS, Kulkarni SK. Differential effect of zileuton, a 5-lipoxygenase inhibitor, against nociceptive paradigms in mice and rats. Pharmacol Biochem Behav. 2005; 81:433–439. [PubMed: 15935457]

Svensson CI, Hua XY, Powell HC, Lai J, Porreca F, Yaksh TL. Prostaglandin E2 release evoked by intrathecal dynorphin is dependent on spinal p38 mitogen activated protein kinase. Neuropeptides. 2005a; 39:485–494. [PubMed: 16176831]

Svensson CI, Hua XY, Protter AA, Powell HC, Yaksh TL. Spinal p38 MAP kinase is necessary for NMDA-induced spinal PGE(2) release and thermal hyperalgesia. Neuroreport. 2003a; 14:1153–1157. [PubMed: 12821799]

Svensson CI, Lucas KK, Hua XY, Powell HC, Dennis EA, Yaksh TL. Spinal phospholipase A2 in inflammatory hyperalgesia: role of the small, secretory phospholipase A2. Neuroscience. 2005b; 133:543–553. [PubMed: 15885922]

Svensson CI, Marsala M, Westerlund A, et al. Activation of p38 mitogen-activated protein kinase in spinal microglia is a critical link in inflammation-induced spinal pain processing. J Neurochem. 2003b; 86:1534–1544. [PubMed: 12950462]

Svensson CI, Yaksh TL. The spinal phospholipase-cyclooxygenase-prostanoid cascade in nociceptive processing. Annu Rev Pharmacol Toxicol. 2002; 42:553–583. [PubMed: 11807183]

Telleria-Diaz A, Ebersberger A, Vasquez E, Schache F, Kahlenbach J, Schaible HG. Different effects of spinally applied prostaglandin D(2) on responses of dorsal horn neurons with knee input in normal rats and in rats with acute knee inflammation. Neuroscience. 2008

Trang T, McNaull B, Quirion R, Jhamandas K. Involvement of spinal lipoxygenase metabolites in hyperalgesia and opioid tolerance. Eur J Pharmacol. 2004; 491:21–30. [PubMed: 15102529]

Tuboly G, Kekesi G, Nagy E, Benedek G, Horvath G. The antinociceptive interaction of anandamide and adenosine at the spinal level. Pharmacol Biochem Behav. 2009; 91:374–379. [PubMed: 18760296]

van Leyen K, Arai K, Jin G, Kenyon V, Gerstner B, Rosenberg PA, Holman TR, Lo EH. Novel lipoxygenase inhibitors as neuroprotective reagents. J Neurosci Res. 2008; 86:904–909. [PubMed: 17960827]

Yang LC, Marsala M, Yaksh TL. Characterization of time course of spinal amino acids, citrulline and PGE2 release after carrageenan/kaolin-induced knee joint inflammation: a chronic microdialysis study. Pain. 1996a; 67:345–354. [PubMed: 8951928]

Yang LC, Marsala M, Yaksh TL. Effect of spinal kainic acid receptor activation on spinal amino acid and prostaglandin E2 release in rat. Neuroscience. 1996b; 75:453–461. [PubMed: 8931009]

Yoo S, Han S, Park YS, Lee JH, Oh U, Hwang SW. Lipoxygenase inhibitors suppressed carrageenan-induced Fos-expression and inflammatory pain responses in the rat. Mol Cells. 2009; 27:417–422. [PubMed: 19390822]

Zarini S, Gijon MA, Folco G, Murphy RC. Effect of arachidonic acid reacylation on leukotriene biosynthesis in human neutrophils stimulated with granulocyte-macrophage colony-stimulating factor and formyl-methionyl-leucyl-phenylalanine. J Biol Chem. 2006; 281:10134–10142. [PubMed: 16495221]

Abbreviations

AEA	anandamide
BBB	blood-brain barrier
CSF	cerebrospinal fluid
COX	cyclooxygenase
CYP	cytochrome P450
DHET	dihydroxyeicosatrienoic acid
EET	epoxyeicosatrienoic acid
EA	ethanolamine
FA	fatty acid
FAAH	fatty acid amide hydrolase
GC	gas chromatography
HX	hepoxilin
HEDH	hydroxyeicosanoid dehydrogenase
HETE	hydroxyeicosatetraenoic acid

| **HODE** | hydroxyoctadecaenoic acid |
i.p	intraperitoneal
LOX	lipoxygenase
LC	liquid chromatography
MS	mass spectrometry
MRM	multiple-reaction monitoring
PPAR	peroxisome proliferator activating factor
PG	prostaglandins
SIM	selected ion monitoring
s.c	subcutaneous
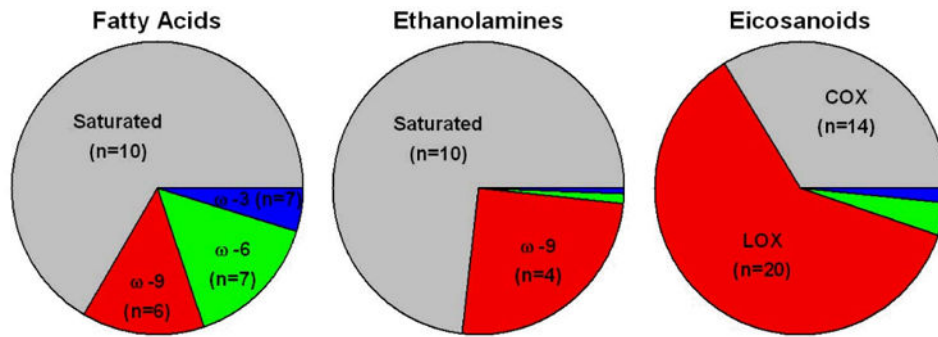
Figure 1. Basal levels of eicosanoids, fatty acids, and ethanolamines in spinal cord tissue
Fatty acid, ethanolamine and eicosanoid lipids were identified and quantitated by mass spectrometry methodology. The size of the pie chart represents the relative mass content of each subclass of lipids, and the number in parenthesis indicates the total species identified. Within the ethanolamines, ω-6 subclass (n=5) is represented in green and ω-3 subclass (n=2) in blue. Withing the eicosanoids, CYP subclass (n=13) is represented in green and non-enzymatic species (n=3) in blue. The complete dataset of individual lipid species are available as supplemental information (Supplemental Table 3-5).
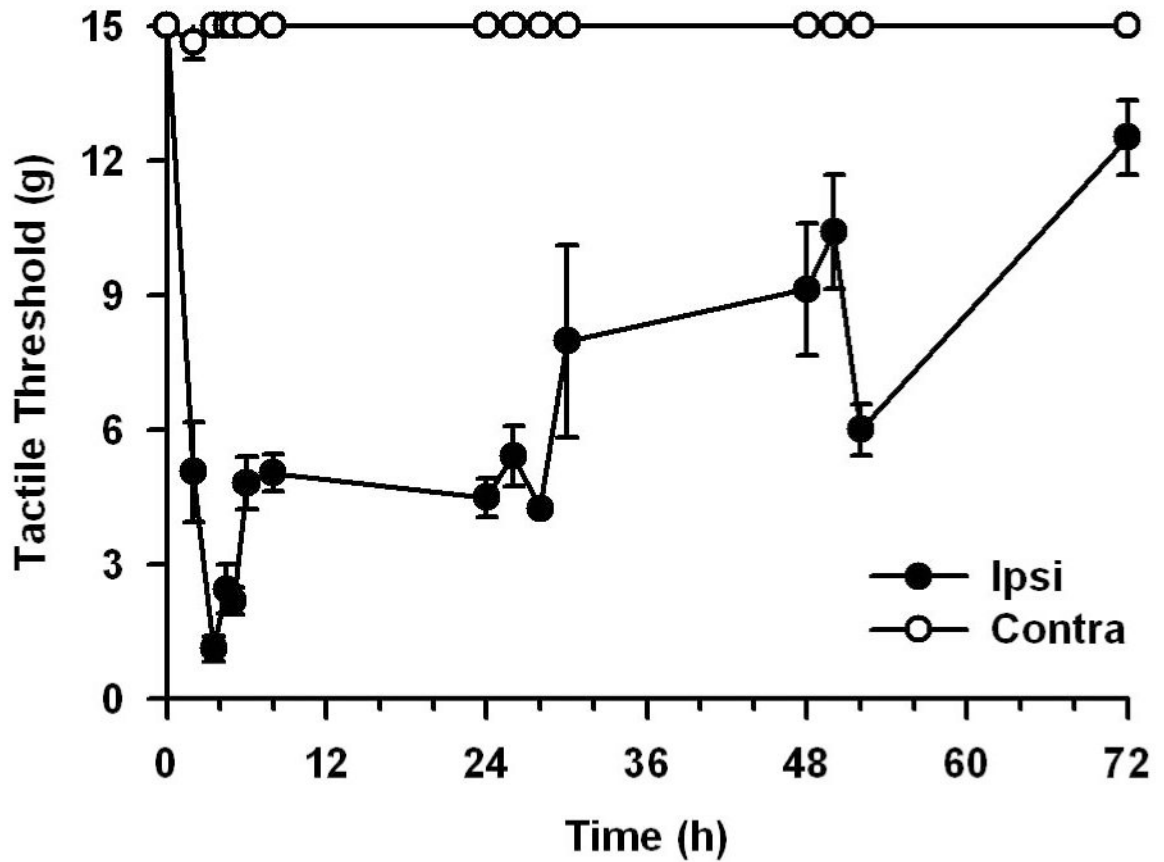
Figure 2. Intraplantar injection of carrageenan induces unilateral tactile allodynia
Naïve rats (n = 4-9) were given an intraplantar injection of 2% carrageenan to the ipsilateral hindpaw, and both the ipsilateral and contralateral hindpaws were tested for nociceptive response by measuring the mechanical withdrawal thresholds for 72 hours.
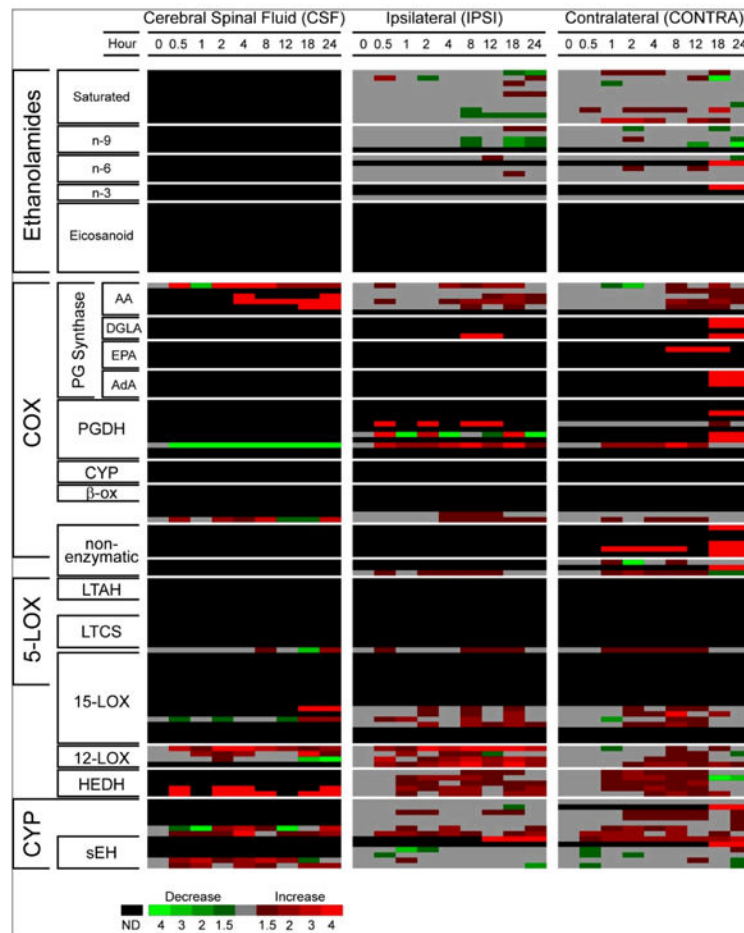
Figure 3. Lipidomic analysis of CSF, ipsilateral and contralateral spinal tissue indicates spinal changes

Heat map representing fold-change in the levels of ethanolamine and eicosanoid lipids species relative to h0 (uninjected) values for cerebral spinal fluid, ipsilateral and contralateral spinal cord from carrageenan injected rats. Increases in metabolite levels are indicated by red, decreases by green, and detectable but unchanged levels by grey. Metabolites below the limit of detection at h0 are indicated by black. n = 4-11 rats/time point/group.
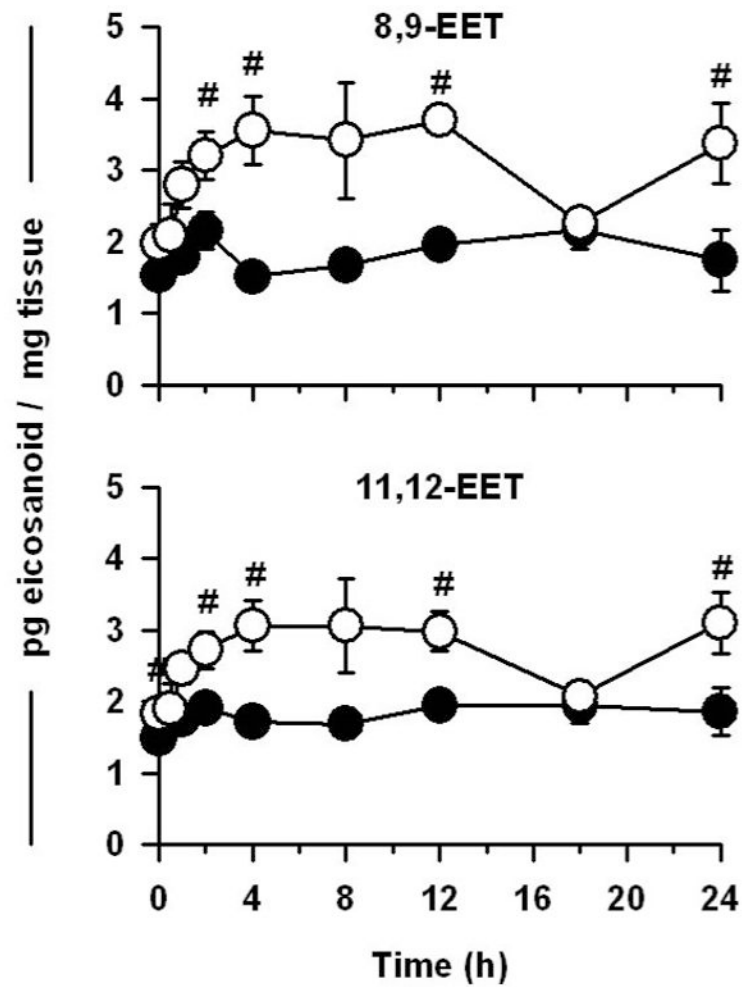
Figure 4. Increased contralateral production of CYP metabolites
Quantitative analysis of lipids in ipsilateral (●) and contralateral (○) spinal cord from carrageenan injected rats. Time course of 8,9-EET and 11,12-EET, expressed as pg of eicosanoid per mg of tissue. ANOVA with simple effects analysis indicated by (#). n = 4-8 rats/time point/group.
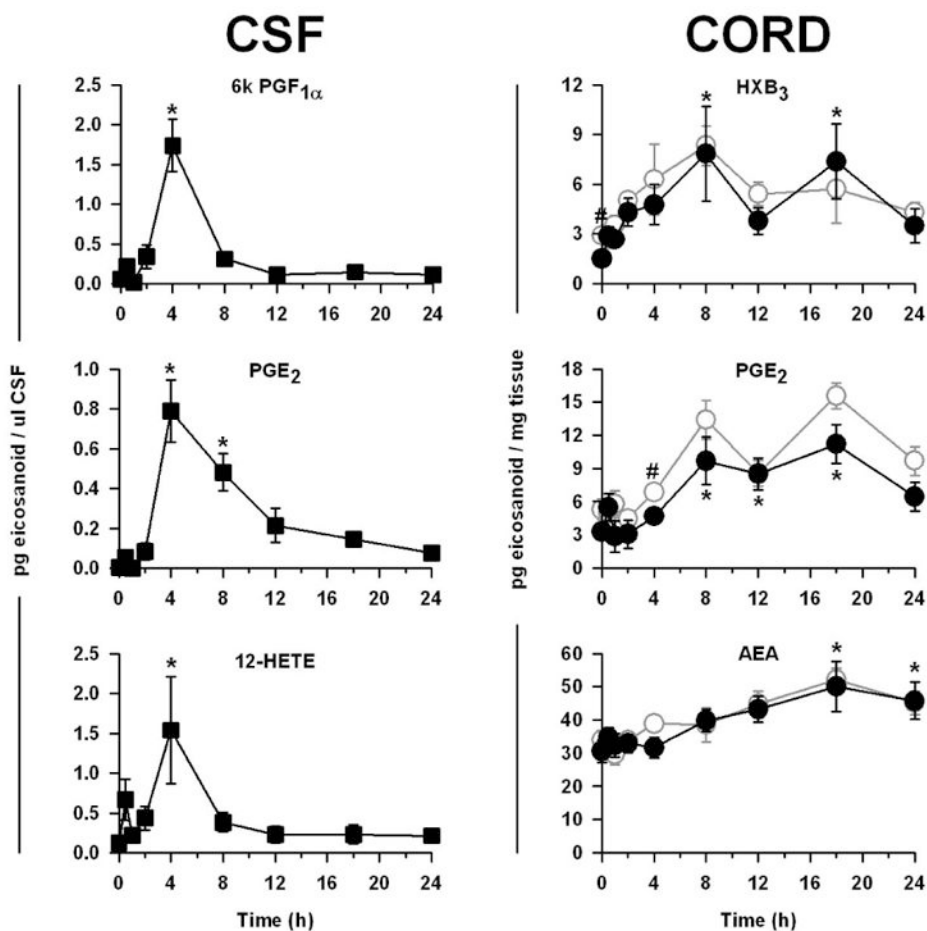
**Figure 5. Temporal production of COX, LOX, and ethanolamide lipid metabolites**
Quantitative analysis of lipids in cerebral spinal fluid (■), ipsilateral (●) and contralateral (○) spinal cord from carrageenan injected rats. Time course of 6k PGF$_{1\alpha}$, PGE$_2$, and 12-HETE in CSF, expressed as pg of eicosanoid per μl of CSF. Time course of HXB$_3$, PGE$_2$, and AEA in ipsilateral spinal cord, expressed as pg of eicosanoid per mg of tissue. ANOVA followed by Dunnett's posthoc (versus time 0 h) for CSF or ipsilateral indicated by (*), and simple effects analysis of ipsilateral vs. contralateral (○) tissue for a given time point indicated by (#). n = 4-11 rats/time point/group.
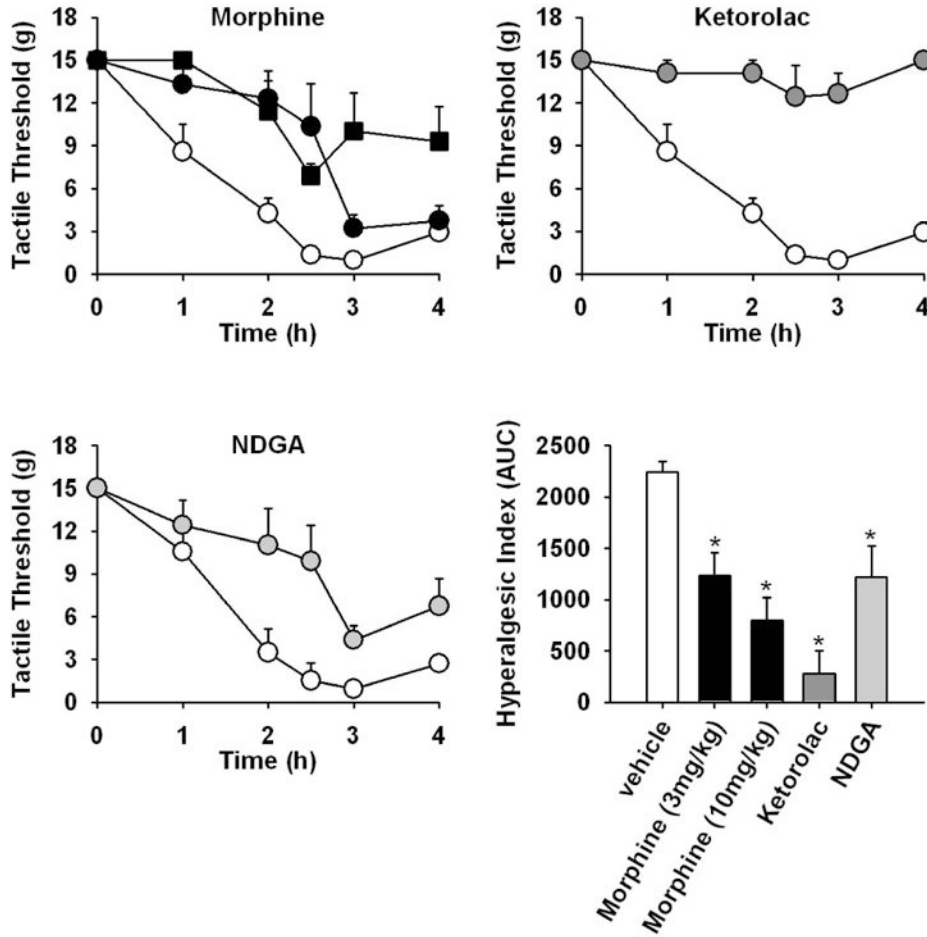
Figure 6. Systemic pretreatment with morphine, ketorolac, or NDGA reduces tactile allodynia
Rats were systemically pretreated 30 minutes prior to intraplantar carrageenan injection with either vehicle (○), morphine (3mg/kg (●) or 10 mg/kg (■), s.c.), ketorolac (30 mg/kg (●), i.p.), or NDGA (10 mg/kg (●), i.p.). Tactile threshold was measured in the ipsilateral hindpaw from 0 to 4 hours, and the hyperalgesic index was determined by measuring the area under the tactile threshold curve. n = 5-6 rats/time point/group.
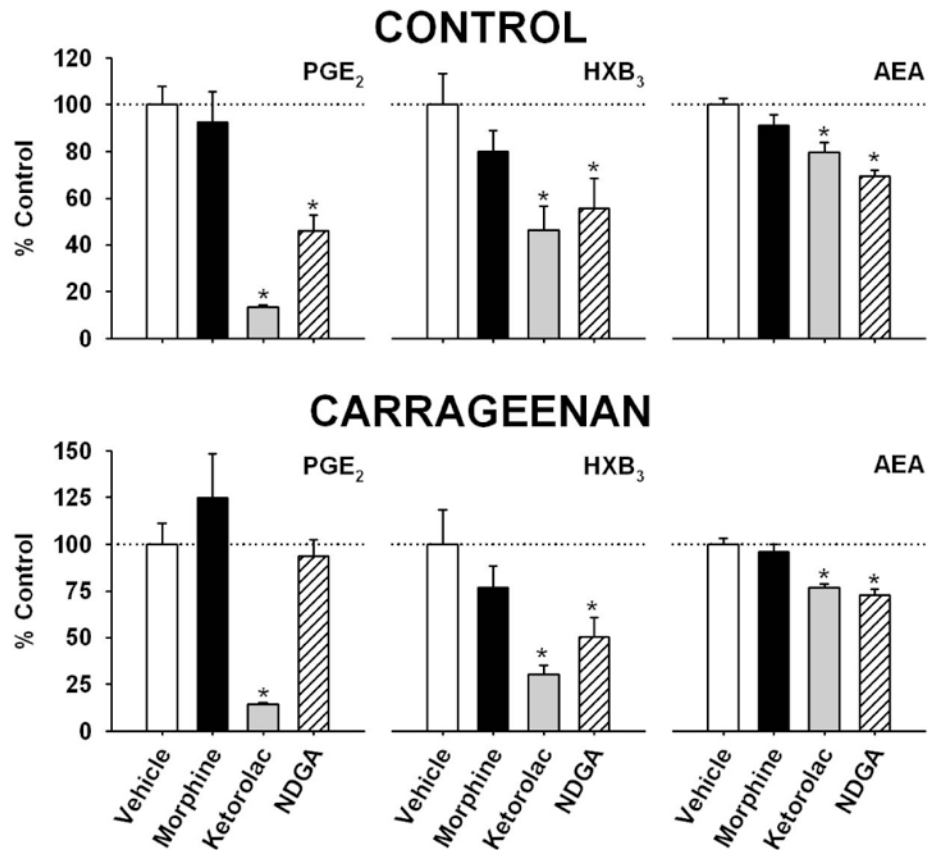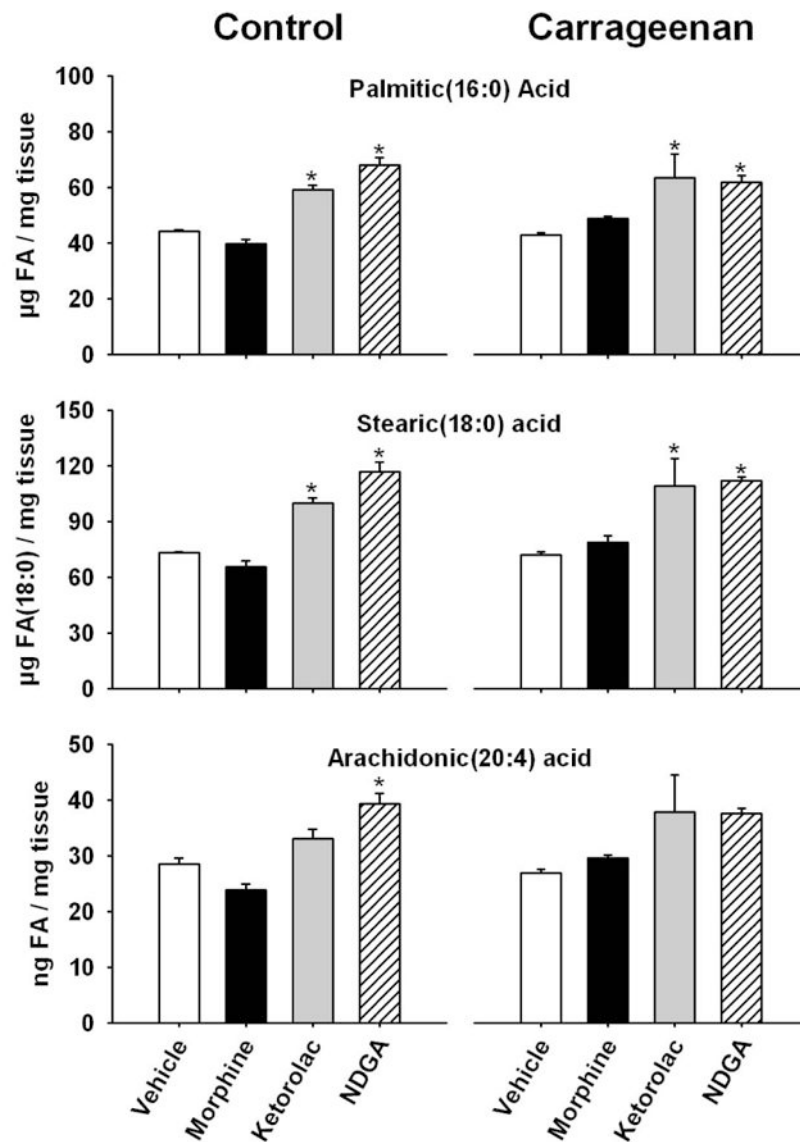
Figure 7. Effect of systemic morphine, ketorolac and NDGA treatment on PGE$_2$, HXB$_3$, and AEA levels

Rats were given vehicle, morphine (3mg/kg or 10 mg/kg, s.c.), ketorolac (30 mg/kg, i.p.), or NDGA (10 mg/kg, i.p.) both 30 minutes prior and 4 hours following intraplantar injection of carrageenan. Spinal cords were removed at 8 hours, and analyzed for PGE$_2$, HXB$_3$, and AEA levels. n = 5-6 rats/time point/group.
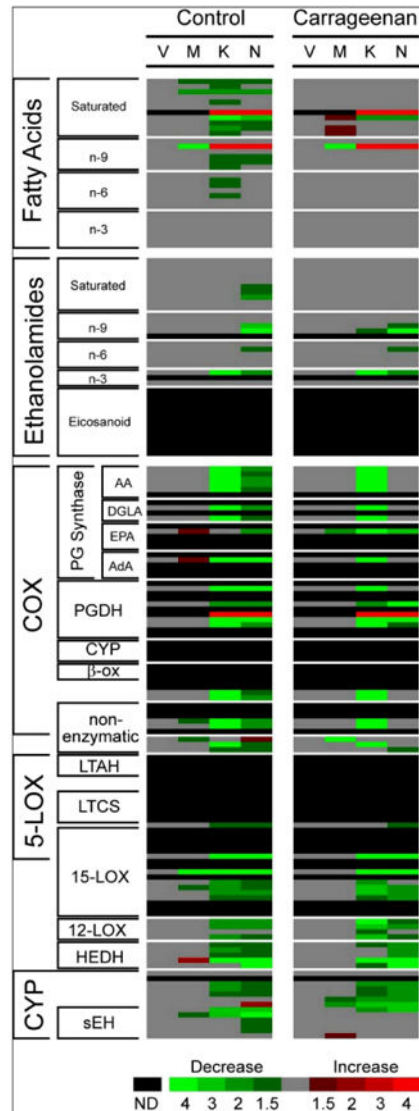
Figure 8. Lipidomic analysis of the global effect of morphine, ketorolac and NDGA treatment in the spinal cord

Heat map representing fold-change in the levels of fatty acid, ethanolamine and eicosanoid lipids species relative to vehicle treated animals. Rats were given vehicle, morphine (3mg/kg or 10 mg/kg, s.c.), ketorolac (30 mg/kg, i.p.), or NDGA (10 mg/kg, i.p.) both 30 minutes prior and 4 hours following intraplantar injection of carrageenan. Spinal cords were removed at 8 hours for lipidomic analyses. n = 5-6 rats/time point/group.

Figure 9. Effect of morphine, ketorolac and NDGA treatment on palmitic, stearic and arachidonic acid levels
Rats were given vehicle, morphine (3mg/kg or 10 mg/kg, s.c.), ketorolac (30 mg/kg, i.p.), or NDGA (10 mg/kg, i.p.) both 30 minutes prior and 4 hours following intraplantar injection of carrageenan. Spinal cords were removed at 8 hours, and analyzed for fatty acid levels. n = 5-6 rats/time point/group.

Table 1

MANOVA analysis of lipidomic changes in CSF and spinal cord

Metabolic Pathways	CSF vs. time	Ipsi vs. time	Contra vs. time	Ipsi vs. Contra
Ethanolamines				
Saturated	-	**0.001**	**0.035**	**0.017**
ω-9	-	0.189	0.178	0.717
ω-6	-	**0.001**	**0.000**	0.604
ω-3	-	**0.018**	**0.025**	0.573
Eicosanoids				
COX	**0.000**	**0.035**	**0.000**	0.987
5-LOX	-	0.207	0.068	0.178
12-LOX	0.341	**0.001**	**0.002**	0.973
15-LOX	0.250	**0.036**	**0.019**	0.761
CYP	0.605	**0.001**	**0.002**	**0.004**
non-enzymatic	-	0.085	**0.002**	0.864

Lipidomic array data was analyzed for potential lipid subclass changes by multivariate analysis of variance (MANOVA) using Hotelling's T statistic. The p-value for the effect of time on lipid species changes within each subclass for CSF, ipsilateral, and contralateral was used to identify temporal changes within each tissue. The p-value for the interaction between time and lipid species changes was used to identify subclass differences between the ipsilateral and contralateral tissue. Significant values (p-value < 0.05) are in bold.